Electrochimica Acta 284 (2018) 1–9

Contents lists available at ScienceDirect

Electrochimica Acta

journal homepage: www.elsevier.com/locate/electacta

A long cycle-life Na-Mg hybrid battery with a chlorine-free electrolyte based on $Mg(TFSI)_2$

Jing Zeng, Zulai Cao, Yang Yang, Yunhui Wang, Yueying Peng, Yiyong Zhang, Jing Wang**, Jinbao Zhao*

Collaborative Innovation Center of Chemistry for Energy Materials, State Key Lab of Physical Chemistry of Solid Surfaces, State-Province Joint Engineering Laboratory of Power Source Technology for New Energy Vehicle, College of Chemistry and Chemical Engineering, Xiamen University, Xiamen, 361005, PR China

ARTICLE INFO

Article history:
Received 23 May 2018
Received in revised form
9 July 2018
Accepted 16 July 2018
Available online 23 July 2018

Keywords:
Na-Mg hybrid batteries
$Mg(TFSI)_2$
Chlorine-free
Excellent electrochemical performance

ABSTRACT

The commercial applications of rechargeable magnesium batteries (RMBs) are hindered by the slow diffusion kinetic of Mg^{2+} ions in cathode materials. To overcome this problem, we design a new Na-Mg hybrid battery with the $NaTi_2(PO_4)_3$@Carbon (NTP@C) nanoparticles as a cathode material, the Mg metal as an anode and the $Mg(TFSI)_2 + NaBH_4$ - triglyme/1,2-Dimethoxyethane (DME) as a hybrid electrolyte. For the first time, the $Mg(TFSI)_2$ is applied as a Mg^{2+} ions source in the chlorine-free Na-Mg hybrid electrolyte with $NaBH_4$ as both Na^+ ions source and moisture scavenger. The NTP@C/Mg hybrid battery shows excellent electrochemical performance. The corresponding average capacity decay after 1000 cycles is only 0.004% and 0.008% per cycle at 2 C and 10 C, respectively. Even at 20 C, about 60 mAh g^{-1} can be obtained after 26000 cycles. The impressive capacity retention of 93.7% and 90.2% can be obtained at 5 and 10 C, respectively. The excellent electrochemical performance of the hybrid battery confirms the feasibility using $Mg(TFSI)_2$ in the chlorine-free hybrid electrolyte for long term cycle. The developed NTP@C/Mg hybrid battery possesses the advantages of excellent electrochemical performances, good safety and low cost, making it promising for the commercial applications, especially for the large-scale energy storages.

1. Introduction

The lithium ion batteries (LIBs) have been widely used in our daily life. However, the applications of LIBs in large scale energy storages, such as electric vehicles and grid, are difficult due to the limits of high cost and safety problems [1]. The RMBs have received great attention as one of the post-LIBs due to following several advantages: (i) The deposition of Mg is dendrite-free, making Mg a safe metal anode; (ii) Mg is much cheaper than Li due to its abundant resources in the earth's crust, which is beneficial for decreasing the costs of batteries production; (iii) Mg possesses higher volume energy density (3833 mA h cm^{-3} for Mg metal vs. 2046 mA h cm^{-3} for Li metal) because of its divalent nature [2,3]. However, there are still many challenges in the development of RMBs, among which the sluggish kinetics in cathode is a primary problem. Continually developing and exploring cathode materials is one of the plausible pathways to solve this problem. Nevertheless, due to the strong polarity of divalent Mg^{2+} ions, the diffusion of Mg^{2+} ions in solid materials is very slow, making it difficult to find suitable cathode materials [4,5]. Until now, only a few kinds of cathode materials can serve as Mg^{2+} ions insertion hosts and it is difficult to significantly improve the kinetic of electrodes by merely exploring the cathode materials [4,6]. Developing hybrid batteries by replacing the intercalation of Mg^{2+} ions with Na^+ or Li^+ ions is another feasible and effective way to improve the kinetics of cathode side [7–9]. Compared to Mg^{2+} ions, the intercalation of monovalent ions into cathode materials is much easier. Considering the abundance of Na element, the Na-Mg hybrid batteries are more attractive than the Li-Mg hybrid batteries.

The Na-Mg hybrid batteries, consisting of a Mg metal anode, a Na-intercalated cathode and a Na-Mg hybrid electrolyte, can combine the advantages of the dendrite-free metal anode and fast cathode kinetics process, leading to higher capacity and better rate

---

* Corresponding author.
** Corresponding author.
E-mail addresses: wangjing2015@xmu.edu.cn (J. Wang), jbzhao@xmu.edu.cn (J. Zhao).

https://doi.org/10.1016/j.electacta.2018.07.111
0013-4686/

performance compared to the conventional RMBs [9]. Given that Na-intercalated cathode materials have been intensively investigated and well-established in sodium ion batteries (SIBs), selecting appropriate cathode materials from them is practicable and feasible. Thus, finding suitable hybrid electrolyte is a major task in the Na-Mg hybrid batteries. An ideal electrolyte should meet the requirement of allowing the reversible Mg deposition/stripping at the anode side and providing enough Na^+ ions to insert into the cathode material at the same time. Several types of Na-Mg hybrid batteries have been developed in recent years [9–12]. Kovalenko et al. developed the first Na-Mg hybrid battery constituted by a Mg metal anode, a FeS_2 nanocrystals cathode and a hybrid electrolyte (0.2 M $Mg(BH_4)_2$ + 2 M $NaBH_4$ − diglyme) with the discharge capacity of 189 mAh g^{-1} at 0.2 C, but its cycle performance was poor [9]. Wei et al. reported a TiS_2/Mg hybrid battery based on the similar electrolyte [11]. Despite the excellent cycle performance, only 49% and 34% of the capacity can be remained at 10 C and 20 C, respectively. Moreover, above two kinds of sulfides/Mg hybrid batteries delivered a low average working voltage of 1 V vs. Mg^{2+}/Mg, leading to the decreasing energy density of batteries. Although high-voltage Na-Mg hybrid batteries, such as $Na_3V_2(PO_4)_3$@C/Mg (~2.6 V) hybrid battery, have been developed, the cycle performance is not yet satisfied since only 81.2% of the capacity can be remained after 50 cycles at 1 C [10,12]. In addition, the chlorine-containing hybrid electrolyte is highly corrosive to the current collector and batteries components (stainless steel) [13]. To cope with the corrosive problem, the anti-corrosive current collectors such as Mo and tubular cells are chosen to test the electrochemical performances, which undoubtedly will increase the batteries production cost [14]. Thus, there are still serious challenges in the high-voltage Na-Mg hybrid battery system under the consideration of both basic researches and commercial applications.

The $Mg(TFSI)_2$ is a promising candidate of Mg salts for the chlorine-free high-voltage hybrid electrolyte due to its high anodic stability (~3.5 V vs. Mg^{2+}/Mg), chemical stability and solubility in organic solvents. To the best of our knowledge, when using Mg metal as an anode, the $Mg(TFSI)_2$ has rarely been used in the chlorine-free electrolyte for hybrid batteries or conventional RMBs for long term cycle [15–19]. One of the prime reasons is that reversible Mg deposition/stripping in $Mg(TFSI)_2$-based electrolyte can only take place in a very strict condition of the H_2O content less than 10 ppm [20,21]. Although the addition of chlorine can effectively improve the electrochemical performance of $Mg(TFSI)_2$-based electrolyte, the serious corrosion problems can not be avoided [18]. Thus, it is important to realize the usage of $Mg(TFSI)_2$ without chlorine for long term cycle. Recently, Douglas etc. reported that Mg could reversibly deposition/stripping in $Mg(TFSI)_2$/tetraglyme by adding a small amount of $Mg(BH_4)_2$. The important role of $Mg(BH_4)_2$ is to react with impurities in the electrolyte, especially H_2O, to make Mg deposition/stripping possible [22]. Inspired by this work, we design a new hybrid electrolyte by replacing $Mg(BH_4)_2$ with $NaBH_4$ for the Na-Mg hybrid batteries. The $NaBH_4$ plays a key role in two aspects: (i) Similar to $Mg(BH_4)_2$, the $NaBH_4$ can remove the impurities in the electrolyte due to its strong reducibility; (ii) The $NaBH_4$ serves as Na^+ ions source providing sufficient Na^+ ions to insert into the cathode.

In this work, a new Na-Mg hybrid battery with NTP@C nanoparticles as a cathode and Mg metal as an anode has been built (Scheme 1). The $Mg(TFSI)_2$-based dual-salt electrolyte with the $NaBH_4$ as both moisture scavenger and Na^+ ions source in glymes has been developed as a new chlorine-free hybrid electrolyte. The NTP@C/Mg hybrid battery shows excellent cycle performance, rate ability and good safety. The excellent electrochemical performance of the hybrid battery confirms the feasibility using $Mg(TFSI)_2$ in chlorine-free hybrid electrolyte for long term cycle.

2. Experimental part

2.1. Preparation and characterizations of the hybrid electrolyte

The $Mg(TFSI)_2$ (Alfa Aesar) was dried in vacuum oven at 250 °C for 1 h before used. Both triglyme and DME are battery grade. Typically, 0.35 g $Mg(TFSI)_2$ and 0.114 g $Na(BH)_4$ (Shanghai Aladdin Bio-Chem Technology Co., Ltd) were dissolved in 3 mL triglyme or triglyme/DME (volume: volume = 1: 1) under continuous stirring overnight. A quantity of bubbles could be seen due to the production of H_2 from the reaction of $NaBH_4$ with H_2O. Finally, a transparent hybrid electrolyte was obtained. The H_2O content of the $Mg(TFSI)_2$/triglyme electrolyte was measured by using Metrohm 831 Coulometric Karl Fischer titrator. Due to the strong reducibility of $NaBH_4$, the H_2O content of the electrolyte with $NaBH_4$ could not be measured. The cyclic voltammetry (CV) curves and linear sweep voltammetry (LSV) curve of the electrolyte were measured in a three-electrode system with Pt as a working electrode and fresh-polished Mg as both counter and reference electrode. The deposition of the hybrid electrolyte was operated at 0.2 mA cm^{-2} for 12 h on Cu substrate. The deposits of the electrolyte were washed with DME several times before tests. To confirm the insertion ions are Na^+ ions, an electrolyte without Na^+ ions (0.2 M $Mg(TFSI)_2$ + 0.1 M $Mg(BH_4)_2$ - triglyme/DME) was prepared, in which the $Mg(BH_4)_2$ serves only as a moisture scavenger. The conductivities of the electrolytes with triglyme and triglyme/DME as the solvents were measured on a Leici conductivity meter DDS-307A.

2.2. Electrochemical measurements of the NTP@C/Mg hybrid battery

The slurry composed of 70 wt% the as-prepared NTP@C, 20 wt% acetylene black, 5 wt% sodium carboxymethylcellulose (CMC) and 5 wt% styrene butadiene rubber (SBR) was casted on a stainless steel mesh and dried at 80 °C in vacuum oven overnight. Details for the preparation and characterizations of the NTP@C can be found in the supporting information. The mass loading of the NTP@C was about 0.8–1.0 mg cm^{-2} for galvanostatic charge-discharge tests and ~2.6 mg cm^{-2} for *ex-situ* XRD measurements. The electrochemical performances were measured by using CR2032 coin-type cells with the Celgard 2400 (25 μm) as the separator and the fresh-polished Mg foil as an anode. The galvanostatic charge-discharge tests of the NTP@C electrodes were performed in the potential range of 0.5–2.1 V vs. Mg^{2+}/Mg at different current densities. The CV test of the batteries was carried out at different scan rates. The cells after cycling (600 cycles for 1 C and 26000 cycles for 20 C) was disassembled in a glove box and the Mg anodes were washed with DME before tests. All the electrochemical measurements were operated at room temperature (25 °C).

3. Results and discussion

3.1. Electrochemical performance of the hybrid electrolyte

To remove the trace H_2O in the $Mg(TFSI)_2$ electrolyte, $NaBH_4$ is an ideal choice. It can serve as a moisture scavenger and Na^+ ions source for hybrid electrolyte at the same time. Thus, no other Na salt is needed. For hybrid electrolyte, the solvent is also an important factor that affects the behavior of Mg deposition. Since Mg can react with polar aprotic solvent (eg. acetonitrile, ethylene carbonate), the ethers (eg. tetrahydrofuran and glymes) are usually used in the RMBs. The glymes with multiple coordinating ether oxygen donors are beneficial to the reversibility of Mg electrochemistry. They can solvate Mg^{2+} ions to form an appropriated solvation

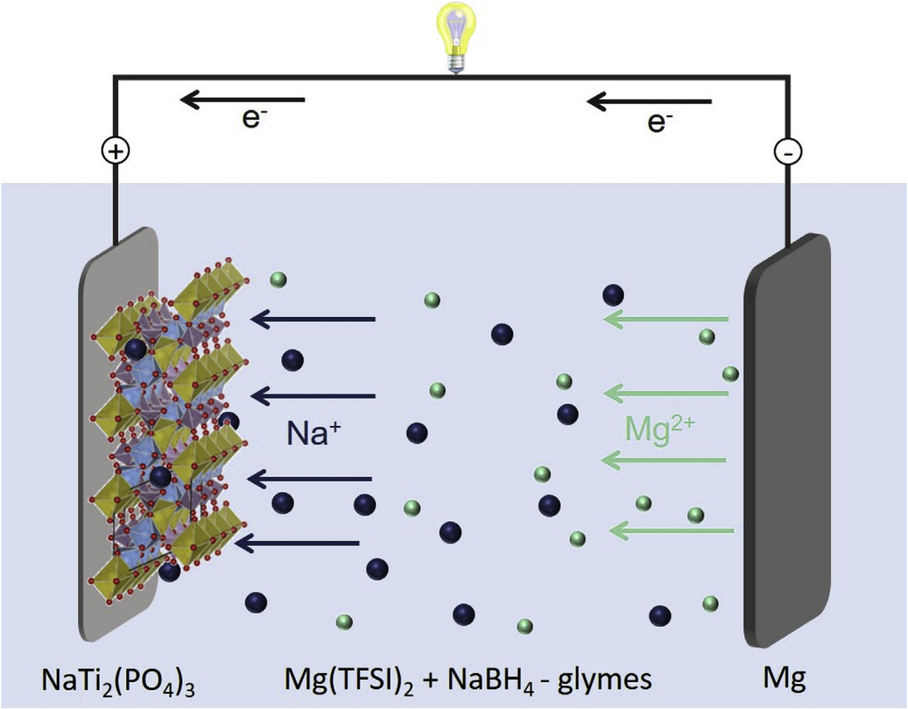

Scheme 1. Illustration of the NTP@C/Mg hybrid battery.

sheath structure for Mg deposition/stripping [23]. Apart from the high solvating power, they also exhibit other advantages, including low volatilization and non-corrosive to current collectors. Triglyme with high boiling point (216 °C) has four oxygen atoms. The $[Mg(triglyme)_2]^{2+}$ complex will be formed in $Mg(TFSI)_2$ - triglyme electrolyte, making triglyme a suitable solvent for $Mg(TFSI)_2$ [24]. Besides, Yoshiharu et al. reported that Mg can deposition/stripping in $Mg(TFSI)_2$ - triglyme electrolyte [15]. Thus, the triglyme is chosen as the solvent in our study. The H_2O content of $Mg(TFSI)_2$ - triglyme electrolyte is about 200 ppm and no Mg deposition is observed due to the existence of H_2O (Fig. S1). After the addition of 1 M $NaBH_4$, obvious Mg reduction/oxidation peaks can be observed (Fig. S2). The reduction onset potential is - 0.51 V vs. Mg^{2+}/Mg with the initial columbic efficiency of 86.7%, which agrees with the previous result [22].

Despite the advantages of triglyme, the high viscosity nature (1.6 cP) is not beneficial for the ions migration in the electrolyte, which will lead to poor electrochemical performances at high current densities, and high working temperature may be needed for the electrochemical performance measurements [15,25]. Thus, a binary mixture solution, in which one has high solvating power and other one has low viscosity, is desired [26]. In this case, low viscosity DME (0.7 cP) with short chain structure is added into the electrolyte (triglyme: DME = 1: 1, volume: volume) [27]. The ionic conductivity increases from 2.89 mS cm^{-1} to 4.12 mS cm^{-1} after the addition of DME. The electrochemical performance of Mg deposition/stripping in 0.2 M $Mg(TFSI)_2$ + 1M $NaBH_4$ - triglyme/DME is shown in Fig. 1. The LSV curve indicates that the anodic stability of the hybrid electrolyte is about 2.1 V vs. Mg^{2+}/Mg (Fig. 1a). The CV curve of the hybrid electrolyte at first cycle is presented in Fig. 1b. The onset potential for Mg deposition/stripping is - 0.44/0.13 V on Pt with a coulombic efficiency of 82.3%. In order to use metal Mg as an anode for the Na-Mg hybrid battery, the dual-salt electrolyte should allow reversible Mg deposition. To verify this, the composition of deposits from the electrolyte is carefully studied. The XRD pattern of the deposits (Fig. 1c) can be well identified to Mg, and no Na signals are observed. The diffraction peaks located at 32.1°, 34.3° and 36.6°, correspond to the (100), (002) and (101) planes of Mg (JCPDS no. 01-089-4896), respectively. Different from the formation of Li/Na dendrites, the Mg deposits present island-like shape with particle size of 20–100 μm (Fig. 1d). The element mapping results (Fig. 1e–h) show strong signals of Mg with negligible Na signals, confirming that the deposits are Mg. The above results indicate that only the deposition of Mg metal can happen in our proposed hybrid electrolyte, suggesting that this hybrid electrolyte can be well used in the Na-Mg hybrid batteries. To the best of our knowledge, this is the first time to use $Mg(TFSI)_2$ in Na-Mg hybrid batteries. By controlling the amount of moisture scavenger and replacing $NaBH_4$ by other Na salt with wider electrochemical window, a chlorine-free high-voltage hybrid electrolyte based on $Mg(TFSI)_2$ can be developed.

3.2. *Electrochemical performance of the NTP@C/Mg hybrid battery*

To build a Na-Mg hybrid battery, the cathode material with excellent electrochemical performance and suitable working voltage is desired. The NTP with Natrium super ionic conductor (NASICON) structure is an attractive electrode material for the SIBs because of its fast Na^+ ions diffusion kinetics and high specific theoretical capacity (133 mAh g^{-1}) [28,29]. It also possesses pronounced thermal and structural stability due to the strong covalent P-O bonds. The small volume changes of NTP during Na^+ ions insertion/extraction contributes to excellent cycle performances [30]. The NTP delivers a discharge platform at 2.1 V vs. Na^+/Na based on the redox reaction of $V^{4+} \leftrightarrow V^{3+}$. When using Mg metal as an anode, the expected platform voltage is about 1.7 V vs. Mg^{2+}/Mg, considering the differential potential of Na^+/Na (- 2.73 V vs. S.H.E) and Mg^{2+}/Mg (- 2.37 V vs. S.H.E), which is suitable for the hybrid electrolyte. Thus, the NTP is chosen as a cathode material for the hybrid battery in our work. The XRD result (Fig. 2a) shows that the obtained NTP@C can be well identified to the NASICON structure $NaTi_2(PO_4)_3$ with R-3c space group (JCPDS No. 33-1296). The

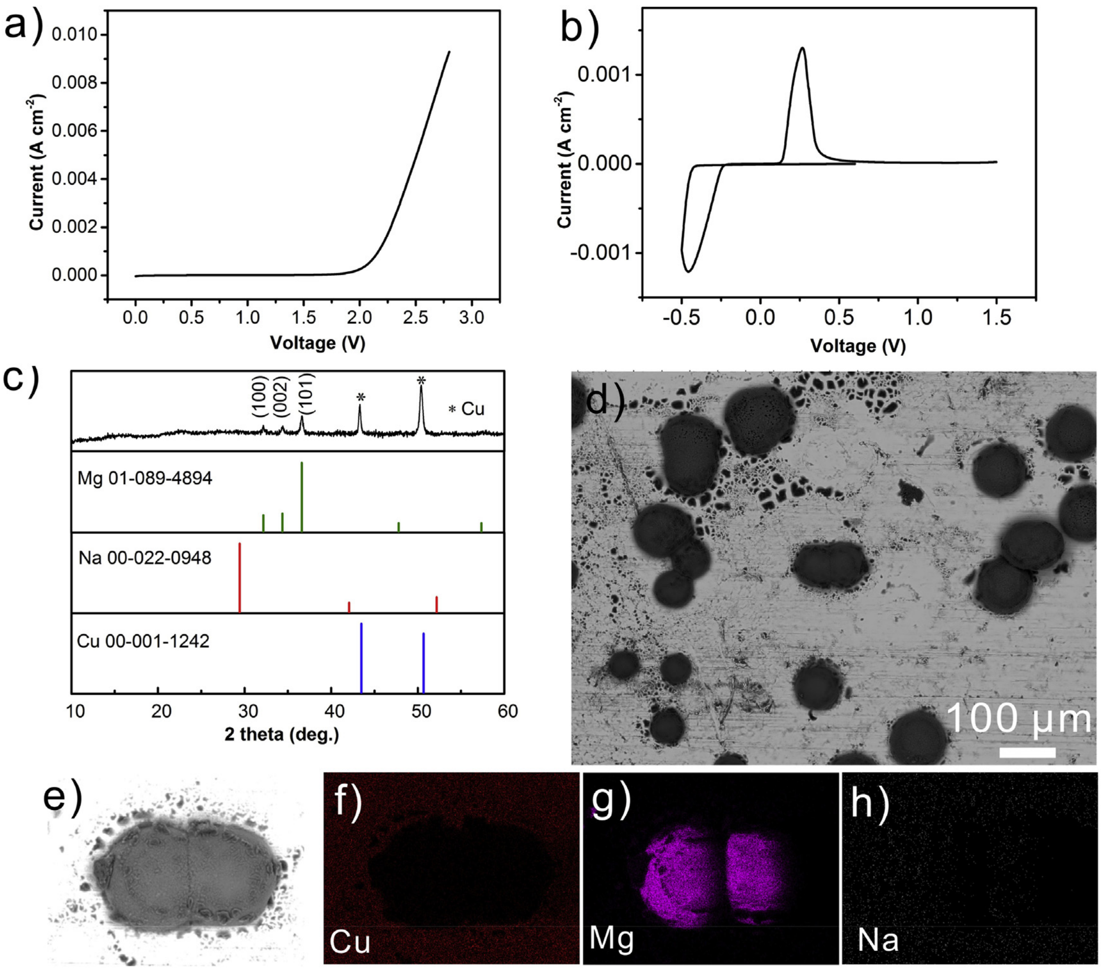

Fig. 1. (a) The LSV curve and (b) CV curve of the 0.2 M $Mg(TFSI)_2$ + 1 M $NaBH_4$ - triglyme/DME electrolyte on Pt working electrode (10 mV s^{-1}); (c) The XRD pattern, (d) The SEM image and (e–h) element mapping of the deposits on Cu substrate.

sucrose serves as a carbon source to improve the electronic conductivity, and the TG curve (Fig. S3a) indicates that the carbon content of the NTP@C is 10.4%. The existence of carbon is further confirmed by the Raman spectra (Fig. S3b). The specific surface area of the NTP@C is measured to be 106.45 $m^2 g^{-1}$ with pore size of around 3 nm and 20–60 nm (Fig. 2b). The morphology and microstructure of the NTP@C have been investigated by SEM and TEM. As shown in Fig. 2c and Fig. S4a, the prepared NTP@C nanoparticles present cubic-like structure with particle size of around 50–100 nm. Mesoporous structure is observed clearly in the particles (Fig. S4b). The HRTEM (Fig. 2d) shows that the NTP crystals are coated with a thin carbon layer of around 10 nm. The interplanar distance of the NTP crystal is measured to be 0.63 nm, corresponding to the d-spacing of (012) planes of the rhombohedral $NaTi_2(PO_4)_3$. The element mapping results (Fig. 2e–f) indicate that all elements are uniformly distributed within the NTP@C particles. The above results indicate that the mesoporous NTP@C nanoparticles have been successfully prepared. The unique structure of the NTP@C can improve the kinetics process of cathode effectively in two ways: (i) The electrical conductivity of the NTP@C composites is enhanced by the carbon coating; (ii) The mesoporous structure of the NTP@C nanoparticles can shorten the diffusion path of Na^+ ions and is beneficial for the infiltration of the electrolyte.

The NTP@C exhibits excellent electrochemical performances in 0.2 M $Mg(TFSI)_2$+1M $NaBH_4$ -triglyme/DME. Fig. 3a displays the galvanostatic charge-discharge voltage profiles of the NTP@C at 1 C in the potential range of 0.5–2.1 V. As shown, the NTP@C shows a discharge plateau at ~1.28 V and a charge plateau at ~1.76 V in the first cycle, corresponding to the redox reaction of Ti^{4+}/Ti^{3+}. The discharge/charge plateaus locate at 1.31/1.70 V and 1.36/1.66 V at 2nd and 5th cycle, respectively. The redox polarization potential decreases from 0.39 V to 0.3 V, which may result from the infiltration process of the electrolyte into the electrode. After five cycles, the discharge/charge plateaus become relatively stable. Due to the existence of the overpotential for Mg deposition, the discharge plateau of the NTP@C/Mg hybrid batteries (1.36 V) is lower than the expected value (1.7 V). To confirm the role of Na^+ ions in this electrolyte system, another contrast experiment using 0.2 M $Mg(TFSI)_2$ + 0.01 M $Mg(BH_4)_2$ - triglyme/DME has been set (Fig. S5). The NTP@C shows a negligible capacity (6 mAh g^{-1}) in the electrolyte without Na^+ ions, suggesting the difficult intercalation of Mg^{2+} ions into NTP@C. The chemical compositions of the working electrode measured also confirms the Na intercalation process. In addition, the carbon material in the working electrode provides negligible capacity (Fig. S6). Therefore, the capacity is ascribed to the insertion of Na^+ ions. The NTP@C delivers an initial discharge capacity of 112 mAh g^{-1} with the coulombic efficiency of 100.1% at 1 C, indicating that about 1.9 Na^+ ions insert into the $NaTi_2(PO_4)_3$ per unit. The capacity remains at 109.8 mAh g^{-1} after 600 cycles, corresponding to the average capacity decay of only 0.003% per cycle (Fig. 3b). At 2 C, the initial discharge capacity is

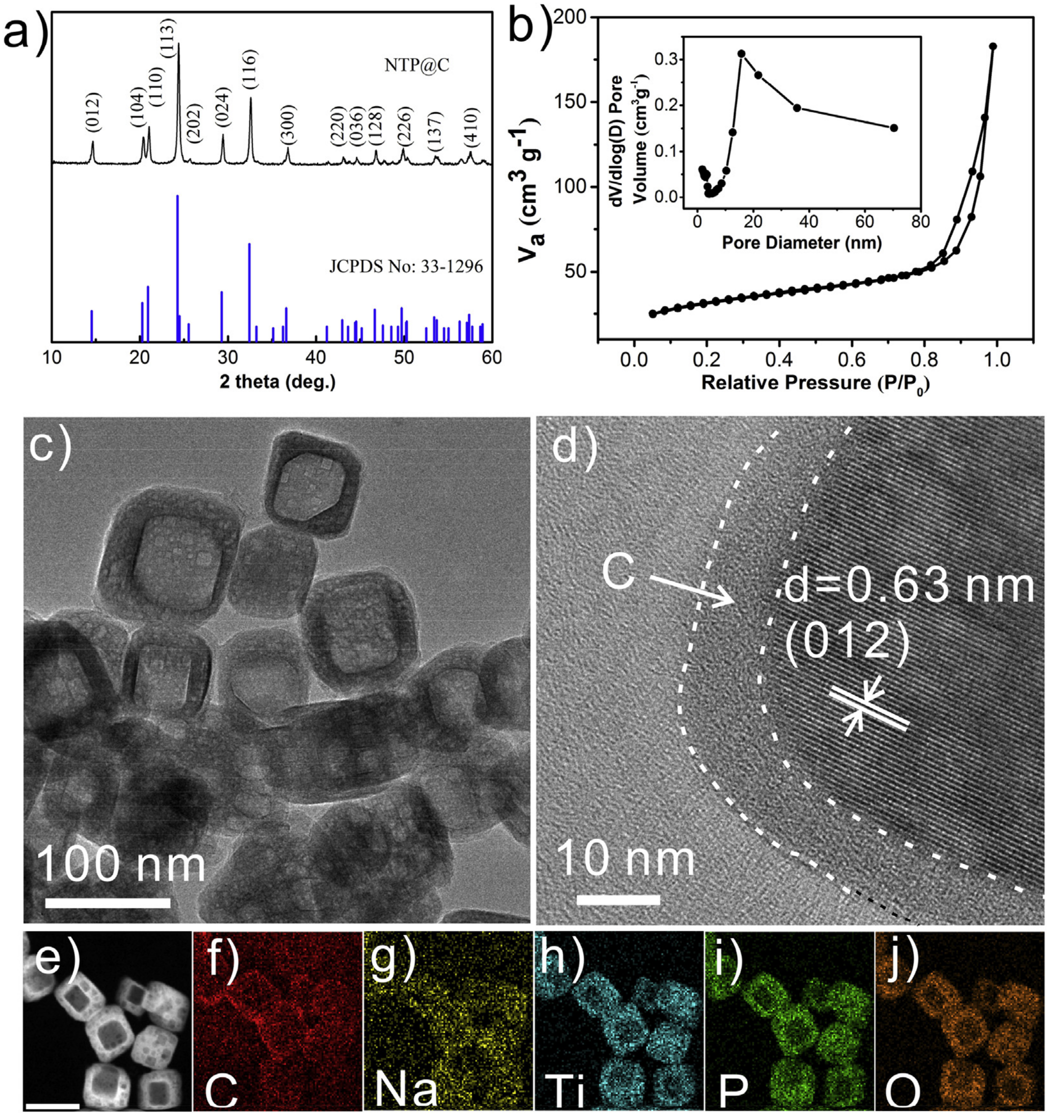

Fig. 2. (a) The XRD pattern, (b) N_2 adsorption/desorption isotherms and the corresponding pore size distribution (insert figure), (c) TEM image, (d) HRTEM, (e) High angle annular dark field (HAADF)-TEM image (The scale bar is 100 nm), and (f–j) the corresponding element mapping of C, Na, Ti, P and O, respectively, of the NTP@C.

110 mAh g^{-1} with the coulombic efficiency of 97.8% (Fig. 3c). About 94.6% of the capacity can be retained after 1000 cycles, corresponding to an average capacity decay of only 0.005% per cycle. When the current density increases to 5 C, the NTP@C delivers a discharge capacity of 101.5 mAh g^{-1} and keeps at 93.7 mAh g^{-1} after 1000 cycles with the coulombic efficiency appropriate to 100% (Fig. 3d). Compared to the electrochemical performance in 0.2 M $Mg(TFSI)_2$ + 1M $NaBH_4$ − triglyme (Fig. S7), the specific capacity and cycle performance are both improved after the addition of DME, especially at high current densities. To confirm the high performance of the developed hybrid electrolyte, the electrochemical performance of the NTP@C in a reference electrolyte [0.1M $Mg(BH_4)_2$ + 1 M $NaBH_4$/triglyme-DME] has also been investigated. The results (Fig. S8) show that the developed electrolyte shows better electrochemical performance than the reference electrolyte, confirming the high performance of the developed Na-Mg hybrid electrolyte.

Fig. 4a displays typical galvanostatic charge-discharge voltage profiles at different current densities. As shown, the obvious discharge/charge plateau from 1 C to 10 C can be seen. The hybrid battery also shows excellent long cycle ability at high current densities. A maximum capacity of 101 mAh g^{-1} can be obtained at 10 C and maintain at 93 mAh g^{-1} after 1000 cycles, corresponding to an average capacity decay of only 0.008% per cycle (Fig. 4b). When the current density increases to 20 C, a capacity of about 60 mAh g^{-1} can be obtained after 26000 cycles (Fig. 4c) and the voltage profiles can still be well maintained (Fig. S9). The capacity retentions at different current densities reflect the rate ability of the hybrid battery. The highest specific capacity is 110, 105, 101 and 67 mAh g^{-1} at 2, 5, 10 and 20 C, corresponding to the capacity retention of 98.2%, 93.7%, 90.2% and 58.9%, respectively. The NTP@C/Mg hybrid battery shows comparable capacity retention compare to the previous reported $Na_3V_2(PO_4)_3$@C/Mg and $FeFe(CN)_6$/Mg hybrid batteries (Fig. S10) [9–12]. The excellent cycle performance and rate ability of the hybrid battery result from the improved electronic conductivity by both carbon coating and intrinsic fast ions diffusion in the NTP (5.12E-15 $cm^2\,s^{-1}$ and 2.06E-15 $cm^2\,s^{-1}$ for the cathodic and anodic process, respectively, as shown in Fig. S11).

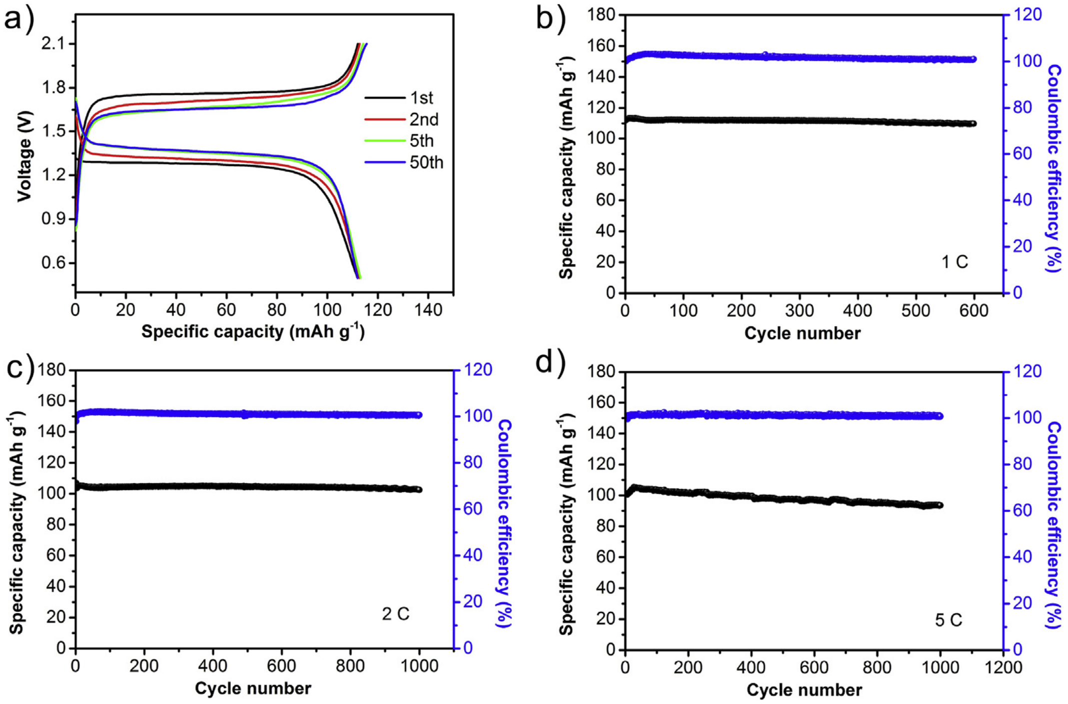

Fig. 3. (a) Galvanostatic charge-discharge voltage profiles of the NTP@C in 0.2 M $Mg(TFSI)_2$ + 1M $NaBH_4$ -triglyme/DME at 1C; The Cycle performance at (b) 1 C, (c) 2 C, and (d) 5 C. All the capacity values are calculated based on the mass of the NTP@C composites (1 C = 133 mAh g^{-1}).

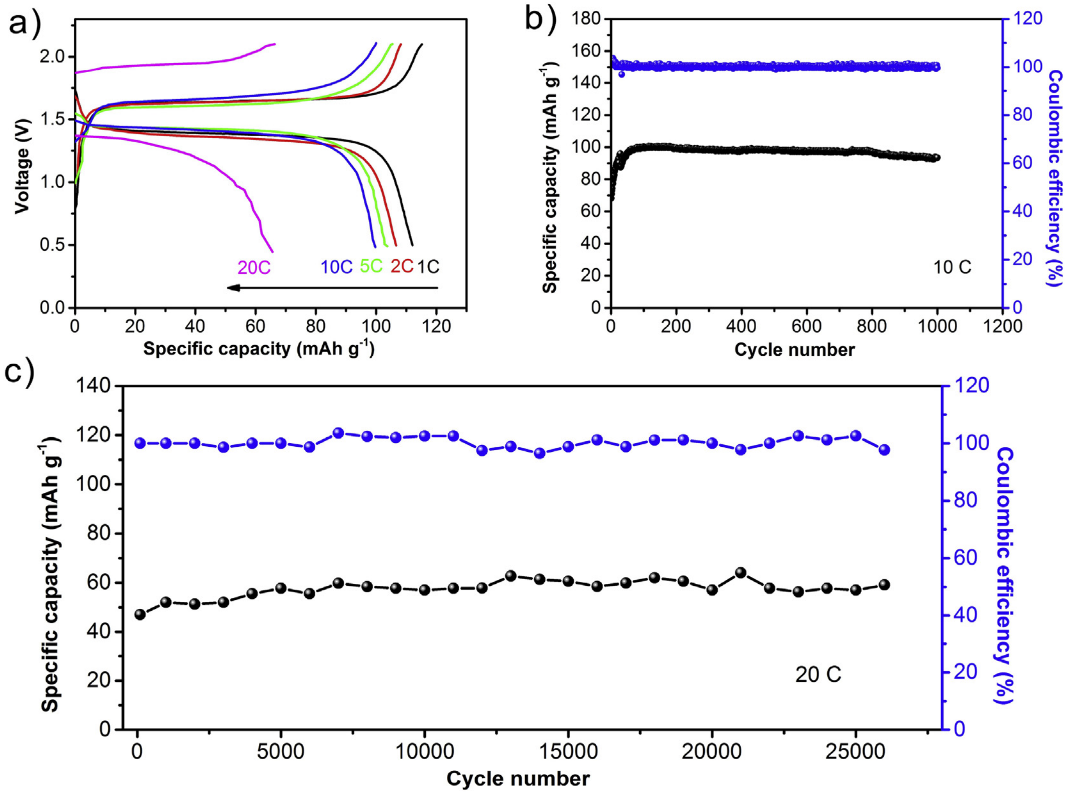

Fig. 4. (a) Typical galvanostatic charge-discharge voltage profiles of the NTP@C in 0.2 M $Mg(TFSI)_2$ + 1M $NaBH_4$ - triglyme/DME at different current densities; Long cycle performance of the NTP@C (b) at 10 C and (c) 20 C after five cycles activation at 1 C.

3.3. Reaction mechanism of the NTP@C/Mg hybrid battery

To investigate the structure change during the electrochemical process, *ex-situ* XRD has been performed at OCV, discharged and charged states in the 2 theta range of 10°–42° (Fig. 5a). At OCV, all the diffraction peaks can be indexed to the rhombohedral $NaTi_2(PO_4)_3$ phase. After fully discharged to 0.5 V, the reflections at 20.26°, 20.92°, 24.24°, 29.28° and 32.44°, corresponding to the diffraction peaks of (104), (110), (113), (024) and (116) planes of $NaTi_2(PO_4)_3$, respectively, disappear. Instead, new peaks at 20.12°, 23.63°, 28.58°, 31.28° and 31.99° appear. The new diffraction patterns can be indexed to the $Na_3Ti_2(PO_4)_3$ phase [31,32]. Compared with the OCV state, the reflections shift to lower angle, indicating that the insertion of Na^+ ions into $NaTi_2(PO_4)_3$ causes the unite cell to expand. During the charge process, the reflections from $Na_3Ti_2(PO_4)_3$ phase disappear and the peaks corresponding to $NaTi_2(PO_4)_3$ phase fully recover. The XRD refinement results of the NTP@C electrode before charge-discharge and charge-discharge after 100 cycles at 1 C (Fig. S12 and Table S2) show that only 0.12% of the volume has changed, indicating the structure of the NTP is rather stable. The microstructure of the NTP@C after 600 cycles at 1 C has also been investigated by the TEM (Fig. 5b and c). As shown, the cubic-like structure of the NTP@C can be well maintained. The interplanar distance is 0.63 nm, corresponding to the (012) planes of the $NaTi_2(PO_4)_3$ phase. The obvious lattice fringe reveals that the NTP is still highly crystalline after 600 cycles, which is consistent with the excellent cycle performance. Thus, according to above analysis, the electrochemical reactions are proposed as follow:

$$\text{Cathode: } NaTi_2(PO_4)_3 + 1.9\,Na^+ + 2\,e^- \leftrightarrow Na_{2.9}Ti_2(PO_3)_4$$

$$\text{Anode: } Mg - 2e^- \leftrightarrow Mg^{2+}$$

3.4. Safety properties of the NTP@C/Mg hybrid battery

Using Na metal as an anode in the SIBs suffers from serious safety problem due to the dendrite problem [33]. One of the advantages of the Na-Mg hybrid batteries is to utilize Mg metal as the anode with good safety due to its dendrite-free nature. To confirm this, the morphologies of Mg metal anode after cycling at low current density (1 C, ~0.1 mA cm^{-2}) and high current density (20 C, ~2 mA cm^{-2}) have been both studied (Fig. 6). Compared to the fresh-polished Mg (Fig. S13), the surface of Mg cycled at 1 C for 600 cycles is still relatively dense and smooth, which is consistent with previous reports [11]. The Mg anode becomes rather rough with angular structure after cycling at 20 C for 20000 cycles. Since Mg is preferable for hexagonal growth, the morphologies are very different from Na or Li dendrites, which can easily penetrate the separator and cause a short circuit. The NTP@C/Mg hybrid battery can be well cycled more than 20000 cycles using a polypropylene separator of 25 μm thickness, indicating the hybrid battery possesses high safety.

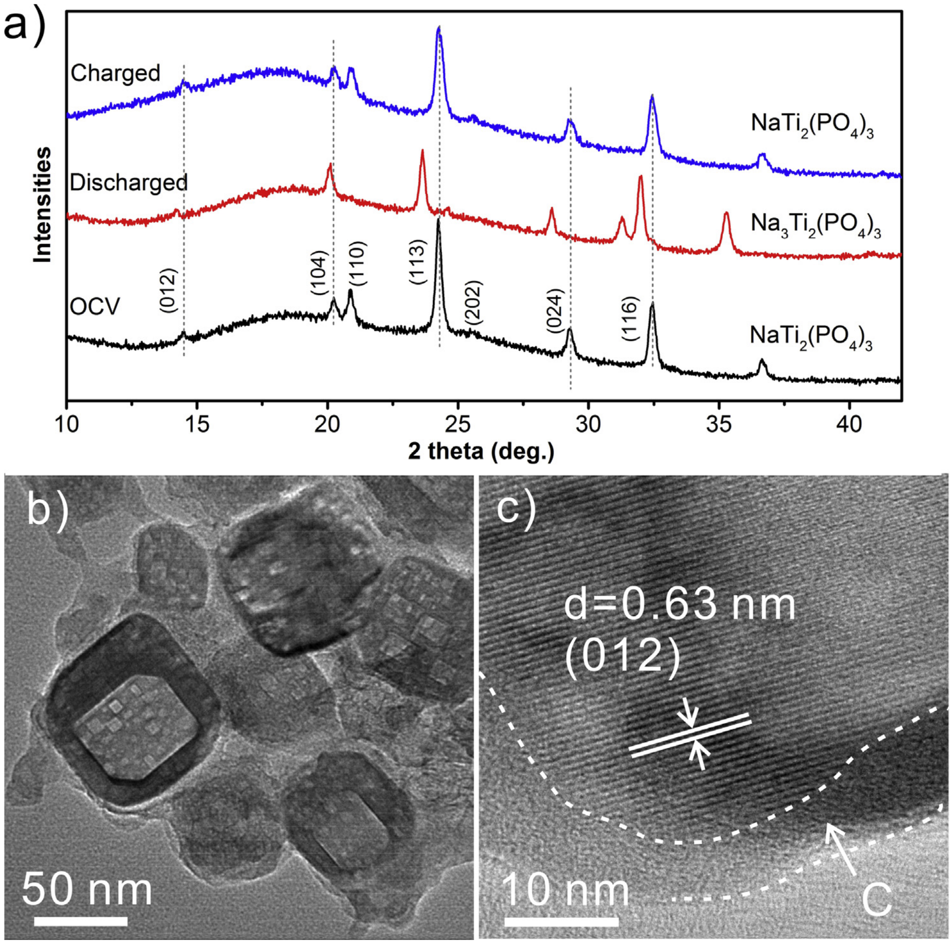

Fig. 5. The *ex-situ* XRD of the NTP@C electrode at OCV, discharged state and charged state, respectively; (b) TEM image and (c) HRTEM image of the NTP@C after 600 cycles at 1 C.

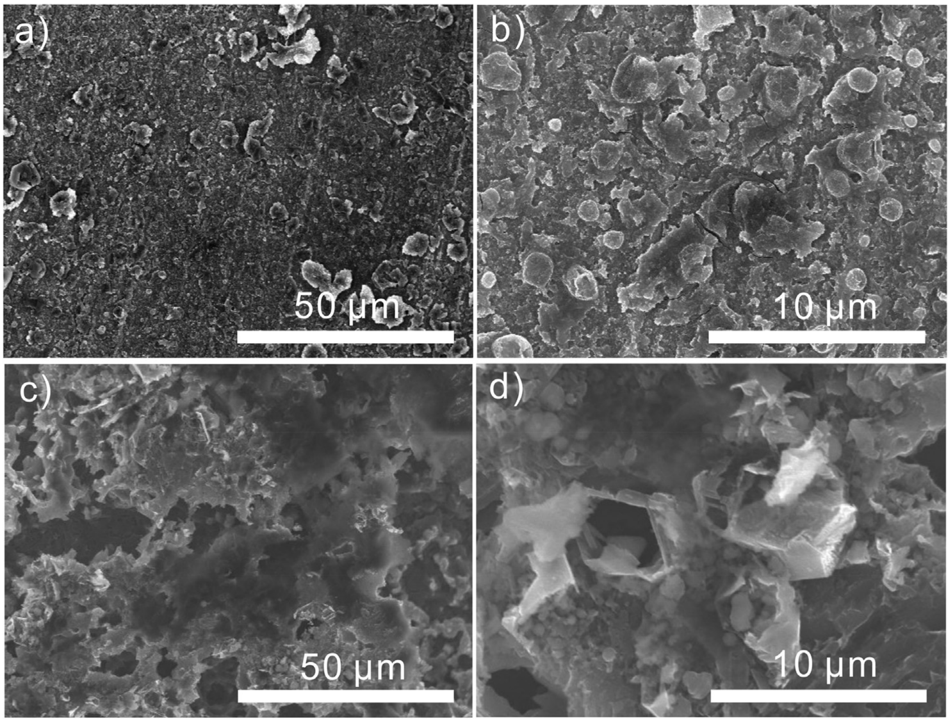

Fig. 6. SEM images of Mg anode after (a, b) 600 cycles at 1 C and (c, d) after 20000 cycles at 20 C, respectively.

4. Conclusions

For the first time, the $Mg(TFSI)_2$ has been applied as a Mg^{2+} ions source in the chlorine-free Na-Mg hybrid electrolyte with the $NaBH_4$ as both the Na^+ ions source and moisture scavenger, and the triglyme/DME as the solvent. Combining with the mesoporous NTP@C nanoparticles as a cathode material and the Mg metal as an anode, a new Na-Mg hybrid battery, NTP@C/Mg, has been built. The hybrid battery shows excellent cycle performances. After 1000 cycles, the corresponding average capacity decay is only 0.004% and 0.008% per cycle at 2 C and 10 C, respectively. Even at 20 C, a specific capacity of about 60 mAh g^{-1} is remained after 26000 cycles. The NTP@C/Mg hybrid battery shows the impressive capacity retention of 93.7% and 90.2% at 5 and 10 C, respectively. The electrochemical performance is superior to the conventional RMBs with Mo_6S_8 as a cathode. The excellent electrochemical performances result from two reasons: (i) For the cathode side, both the unique structure of the cubic-like mesoporous NTP@C nanoparticles and the intrinsic fast ions diffusion in the NTP can effectively improve the kinetics; (ii) For the anode side, the addition of $NaBH_4$ in $Mg(TFSI)_2$-based electrolyte allows reversible Mg deposition/stripping behavior with long term ability. The advantages of the NTP@C/Mg hybrid battery in terms of excellent electrochemical performance, good safety and high energy density, are attractive for commercial applications, especially for the large-scale energy storages. The excellent cycle performance of the hybrid battery confirms the feasibility of using $Mg(TFSI)_2$ in a chlorine-free hybrid electrolyte for long term cycle. By controlling the amount of the moisture scavenger and replacing $NaBH_4$ with other Na salt with wider electrochemical window, a chlorine-free high-voltage hybrid electrolyte based on $Mg(TFSI)_2$ can be developed.

Conflict of interest

The authors declare no conflict of interest.

Acknowledgements

We gratefully acknowledge the financial support of National Natural Science Foundation of China (21621091) and National Key Research and Development Program of China (2017YFB0102000). The authors also thank Prof. D. W. Liao for his valuable suggestions.

Appendix A. Supplementary data

Supplementary data related to this article can be found at https://doi.org/10.1016/j.electacta.2018.07.111.

References

[1] I. Shterenberg, M. Salama, Y. Gofer, E. Levi, D. Aurbach, The challenge of developing rechargeable magnesium batteries, MRS Bull. 39 (2014) 453–460.
[2] H.D. Yoo, I. Shterenberg, Y. Gofer, G. Gershinsky, N. Pour, D. Aurbach, Mg rechargeable batteries: an on-going challenge, Energy Environ. Sci. 6 (2013) 2265–2279.
[3] J. Muldoon, C.B. Bucur, T. Gregory, Quest for nonaqueous multivalent secondary batteries: magnesium and beyond, Chem. Rev. 114 (2014) 11683–11720.
[4] E. Levi, Y. Gofer, D. Aurbach, On the way to rechargeable Mg batteries: the challenge of new cathode materials, Chem. Mater. 22 (2010) 860–868.
[5] E. Levi, M.D. Levi, O. Chasid, D. Aurbach, A review on the problems of the solid state ions diffusion in cathodes for rechargeable Mg batteries, J. Electroceram. 22 (2007) 13–19.
[6] M.M. Huie, D.C. Bock, E.S. Takeuchi, A.C. Marschilok, K.J. Takeuchi, Cathode materials for magnesium and magnesium-ion based batteries, Coord. Chem. Rev. 287 (2015) 15–27.
[7] Y. Cheng, H.J. Chang, H. Dong, D. Choi, V.L. Sprenkle, J. Liu, Y. Yao, G. Li, Rechargeable Mg–Li hybrid batteries: status and challenges, J. Mater. Res. 31 (2016) 3125–3141.
[8] Y.W. Cheng, Y.Y. Shao, J.G. Zhang, V.L. Sprenkle, J. Liu, G.S. Li, High performance batteries based on hybrid magnesium and lithium chemistry, Chem. Commun. 50 (2014) 9644–9646.
[9] M. Walter, K.V. Kraychyk, M. Ibanez, M.V. Koyalenko, Efficient and inexpensive sodium-magnesium hybrid battery, Chem. Mater. 27 (2015) 7452–7458.
[10] H. Dong, Y. Li, Y. Liang, G. Li, C.J. Sun, Y. Ren, Y. Lu, Y. Yao, A magnesium-sodium hybrid battery with high operating voltage, Chem. Commun. 52 (2016) 8263–8266.
[11] X.F. Bian, Y. Gao, Q.A. Fu, S. Indris, Y.M. Ju, Y. Meng, F. Du, N. Bramnik,

H. Ehrenberg, Y.J. Wei, A long cycle-life and high safety Na+/Mg2+ hybrid-ion battery built by using a TiS2 derived titanium sulfide cathode, J. Mater. Chem. A 5 (2017) 600–608.

[12] Y.F. Li, Q.Y. An, Y.W. Cheng, Y.L. Liang, Y. Ren, C.J. Sun, H. Dong, Z.J. Tang, G.S. Li, Y. Yao, A high-voltage rechargeable magnesium-sodium hybrid battery, Nano Energy 34 (2017) 188–194.

[13] J. Muldoon, C.B. Bucur, A.G. Oliver, J. Zajicek, G.D. Allred, W.C. Boggess, Corrosion of magnesium electrolytes: chlorides – the culprit, Energy Environ. Sci. 6 (2013) 482–487.

[14] Y.W. Cheng, T.B. Liu, Y.Y. Shao, M.H. Engelhard, J. Liu, G.S. Li, Electrochemically stable cathode current collectors for rechargeable magnesium batteries, J. Mater. Chem. A 2 (2014) 2473–2477.

[15] Y. Orikasa, T. Masese, Y. Koyama, T. Mori, M. Hattori, K. Yamamoto, T. Okado, Z.D. Huang, T. Minato, C. Tassel, J. Kim, Y. Kobayashi, T. Abe, H. Kageyama, Y. Uchimoto, High energy density rechargeable magnesium battery using earth-abundant and non-toxic elements, Sci. Rep. 4 (2014) 5622.

[16] J. Zeng, Y. Yang, S. Lai, J. Huang, Y. Zhang, J. Wang, J. Zhao, A promising high-voltage cathode material based on mesoporous Na3 V2 (PO4)3/C for rechargeable magnesium batteries, Chemistry 23 (2017) 16898–16905.

[17] T. Gao, S. Hou, F. Wang, Z. Ma, X. Li, K. Xu, C. Wang, Reversible S(0)/MgSx redox chemistry in a MgTFSI2/MgCl2/DME electrolyte for rechargeable Mg/S batteries, Angew. Chem. 56 (2017) 13526–13530.

[18] N. Sa, B. Pan, A. Saha-Shah, A.A. Hubaud, J.T. Vaughey, L.A. Baker, C. Liao, A.K. Burrell, Role of chloride for a simple, non-grignard Mg electrolyte in ether-based solvents, ACS Appl. Mater. Interfaces 8 (2016) 16002–16008.

[19] M. Cabello, R. Alcántara, F. Nacimiento, P. Lavela, M.J. Aragón, J.L. Tirado, Na 3 V 2 (PO 4) 3 as electrode material for rechargeable magnesium batteries: a case of sodium-magnesium hybrid battery, Electrochim. Acta 246 (2017) 908–913.

[20] A. Kitada, Y. Kang, Y. Uchimoto, K. Murase, Room-temperature electrodeposition of Mg metal from amide salts dissolved in glyme-ionic liquid mixture, J. Electrochem. Soc. 161 (2014) D102–D106.

[21] M. Salama, Ivgeni Shterenberg, Hyun Deog Yoo, Gofer Yosef, Jin-Bum Park, Yang-Kook Sun, Doron Aurbach, Evaluation of (CF3SO2)2N– (TFSI) based electrolyte solutions for Mg batteries, J. Electrochem. Soc. 13 (2015) A7118–A7128.

[22] Z. Ma, M. Kar, C.L. Xiao, M. Forsyth, D.R. MacFarlane, Electrochemical cycling of Mg in Mg[TFSI](2)/tetraglyme electrolytes, Electrochem. Commun. 78 (2017) 29–32.

[23] S.H. Lapidus, N.N. Rajput, X. Qu, K.W. Chapman, K.A. Persson, P.J. Chupas, Solvation structure and energetics of electrolytes for multivalent energy storage, Phys. Chem. Chem. Phys. : PCCP 16 (2014) 21941–21945.

[24] T. Kimura, K. Fujii, Y. Sato, M. Morita, N. Yoshimoto, Solvation of magnesium ion in triglyme-based electrolyte solutions, J. Phys. Chem. C 119 (2015) 18911–18917.

[25] A. Ponrouch, E. Marchante, M. Courty, J.-M. Tarascon, M.R. Palacín, In search of an optimized electrolyte for Na-ion batteries, Energy Environ. Sci. 5 (2012) 8572.

[26] S.Y. Ha, Y.W. Lee, S.W. Woo, B. Koo, J.S. Kim, J. Cho, K.T. Lee, N.S. Choi, Magnesium(II) bis(trifluoromethane sulfonyl) imide-based electrolytes with wide electrochemical windows for rechargeable magnesium batteries, ACS Appl. Mater. Interfaces 6 (2014) 4063–4073.

[27] A. Kitada, Y. Kang, Y. Uchimoto, K. Murase, Room-temperature electrodeposition of Mg metal from amide salts dissolved in glyme-ionic liquid mixture, J. Electrochem. Soc. 161 (2013) D102–D106.

[28] C. Wu, P. Kopold, Y.L. Ding, P.A. van Aken, J. Maier, Y. Yu, Synthesizing porous NaTi2(PO4)3 nanoparticles embedded in 3D graphene networks for high-rate and long cycle-life sodium electrodes, ACS Nano 9 (2015) 6610–6618.

[29] G. Yang, H. Song, M. Wu, C. Wang, Porous NaTi2(PO4)3 nanocubes: a high-rate nonaqueous sodium anode material with more than 10 000 cycle life, J. Mater. Chem. A 3 (2015) 18718–18726.

[30] Y. Jiang, J. Shi, M. Wang, L. Zeng, L. Gu, Y. Yu, Highly reversible and ultrafast sodium storage in NaTi2(PO4)3 nanoparticles embedded in nanocarbon networks, ACS Appl. Mater. Interfaces 8 (2016) 689–695.

[31] C. Xu, Y.N. Xu, C.J. Tang, Q.L. Wei, J.S. Meng, L. Huang, L. Zhou, G.B. Zhang, L. He, L.Q. Mai, Carbon-coated hierarchical NaTi2(PO4)(3) mesoporous microflowers with superior sodium storage performance, Nano Energy 28 (2016) 224–231.

[32] Z. Li, D.B. Ravnsbæk, K. Xiang, Y.-M. Chiang, Na3Ti2(PO4)3 as a sodium-bearing anode for rechargeable aqueous sodium-ion batteries, Electrochem. Commun. 44 (2014) 12–15.

[33] M.D. Slater, D. Kim, E. Lee, C.S. Johnson, Sodium-ion batteries, Adv. Funct. Mater. 23 (2013) 947–958.